Video Article

Solid Lipid Nanoparticles (SLNs) for Intracellular Targeting Applications

Xiomara Calderón-Colón[1], Giorgio Raimondi[2], Jason J. Benkoski[1], Julia B. Patrone[3]

[1]Research and Exploratory Development Department, The Johns Hopkins Applied Physics Laboratory

[2]Department of Plastic and Reconstructive Surgery, Johns Hopkins School of Medicine

[3]Asymmetric Operations Sector, The Johns Hopkins Applied Physics Laboratory

Correspondence to: Julia B. Patrone at julia.patrone@jhuapl.edu

URL: http://www.jove.com/video/53102
DOI: doi:10.3791/53102

Keywords: Bioengineering, Issue 105, Solid Lipid Nanoparticles, Intracellular Targeting, Fibroblasts, Dendritic Cells, Nanobiotechnology

Date Published: 11/17/2015

Citation: Calderón-Colón, X., Raimondi, G., Benkoski, J.J., Patrone, J.B. Solid Lipid Nanoparticles (SLNs) for Intracellular Targeting Applications. *J. Vis. Exp.* (105), e53102, doi:10.3791/53102 (2015).

Abstract

Nanoparticle-based delivery vehicles have shown great promise for intracellular targeting applications, providing a mechanism to specifically alter cellular signaling and gene expression. In a previous investigation, the synthesis of ultra-small solid lipid nanoparticles (SLNs) for topical drug delivery and biomarker detection applications was demonstrated. SLNs are a well-studied example of a nanoparticle delivery system that has emerged as a promising drug delivery vehicle. In this study, SLNs were loaded with a fluorescent dye and used as a model to investigate particle-cell interactions. The phase inversion temperature (PIT) method was used for the synthesis of ultra-small populations of biocompatible nanoparticles. A 3-(4,5-dimethylthiazol-2-yl)-2,5-diphenylphenyltetrazolium bromide (MTT) assay was utilized in order to establish appropriate dosing levels prior to the nanoparticle-cell interaction studies. Furthermore, primary human dermal fibroblasts and mouse dendritic cells were exposed to dye-loaded SLN over time and the interactions with respect to toxicity and particle uptake were characterized using fluorescence microscopy and flow cytometry. This study demonstrated that ultra-small SLNs, as a nanoparticle delivery system, are suitable for intracellular targeting of different cell types.

Video Link

The video component of this article can be found at http://www.jove.com/video/53102/

Introduction

Nanoparticle-based delivery vehicles have shown great promise for intracellular targeting applications, providing a mechanism to specifically alter cellular signaling and gene expression. These vehicles can be loaded with drugs, proteins, and nucleic acids designed to impact cellular responses and achieve a desired effect in target tissues. Many types of nanocarriers have been explored for therapeutic and diagnostic benefit including lipids, polymers, silicon, and magnetic materials. These systems are attractive due to their potential for localized drug delivery, increased therapeutic concentration in target tissues, and reduction of systemic toxicity.

Solid lipid nanoparticles (SLNs) are a well-studied example of a nanoparticle delivery system that has emerged as a promising drug delivery vehicle in recent years. SLNs can be readily formulated for multiple applications including bio-sensing [1], cosmetics [2], and therapeutic delivery [3-7]. Their utility stems from the fact that they are comprised entirely of resorbable, nontoxic lipids, resulting in enhanced biocompatibility. During synthesis, lipophilic drugs can be incorporated into SLN vehicles, thereby increasing drug solubility and suitability for parenteral administration. SLN vehicles also help to stabilize encapsulated therapeutics, reducing their degradation and clearance, and maximizing therapeutic action. These vehicles are particularly well suited for long acting, controlled-release preparations due to their stability at body temperature [3,4,8,9]. Importantly, encapsulation of drugs in lipid nanoparticles alters the intrinsic pharmacokinetic profiles of the drug molecules. This provides a potential advantage by allowing the controlled release of drugs with a narrow therapeutic index. The release rate of SLN-incorporated therapeutics can be tuned based on the lipid degradation rate or the drug diffusion rate in the lipid matrix.

SLNs are often engineered to accumulate in specific target tissues. For example, their size (typically greater than 10 nm) potentiates retention in the circulation, where the leaky vasculature of tumor tissue facilitates deposition. In addition, the route of particle administration has been shown to alter biodistribution with the potential to target specific physiological structures such as lymph nodes [10,11]. Upon deposition in target tissues, achieving appropriate cellular interactions and eventual internalization of nanoparticles is challenging due to the ability of cell membranes to selectively control the flow of ions and molecules into and out of the cell [12]. To facilitate cellular uptake, it is possible to modify nanocarriers with specific ligands including peptides, small molecules, and monoclonal antibodies[13,14]. Several mechanisms including both passive penetration and active transport of nanoparticles across the cell membrane have been previously described [3,12,15]. In general, it has been demonstrated that cell-nanoparticle interactions are influenced by the physicochemical properties of the nanoparticles including size, shape, surface charge and surface chemistry, in addition to cell-specific parameters such as cell type or cell cycle phase [12].

A previous investigation demonstrated the synthesis of sub-10 nm SLNs for topical [16] and biomarker detection applications [1] using the phase inversion temperature (PIT) method [17]. This is a gentle synthesis method where [2] the composition remains constant while the temperature is gradually changed. Continuous stirring of the heated solution, as it cools to RT results in a nanoemulsion. This process results in the synthesis

of SLNs with smaller particle size[1] than that previously reported using various methods for the synthesis of lipid nanoparticles[17-22]. The resulting size scale, less than 20 nm, provides an advantage for intracellular targeting applications due to increased surface area and the potential for enhanced cellular interactions.

A schematic of SLNs, designed to deliver a fluorescent dye or therapeutic, is shown in **Figure 1**. The SLNs consist of a lipid interior (*e.g.*, linear alkane) allowing the incorporation of lipophilic compounds (*e.g.*, dyes or therapeutics) and a surfactant exterior (*e.g.*, linear nonionic surfactant) surrounded by water. In this study, SLNs were loaded with a fluorescent dye and used as a model to investigate particle-cell interactions. Primary human dermal fibroblasts and mouse dendritic cells were exposed to dye-loaded SLN over time in order to characterize interactions with respect to toxicity and particle uptake. A 3-(4,5-dimethylthiazol-2-yl)-2,5-diphenylphenyltetrazolium bromide (MTT) assay was utilized in order to establish appropriate dosing levels. Fluorescence microscopy and flow cytometry were two methods employed to examine particle uptake *in vitro*.

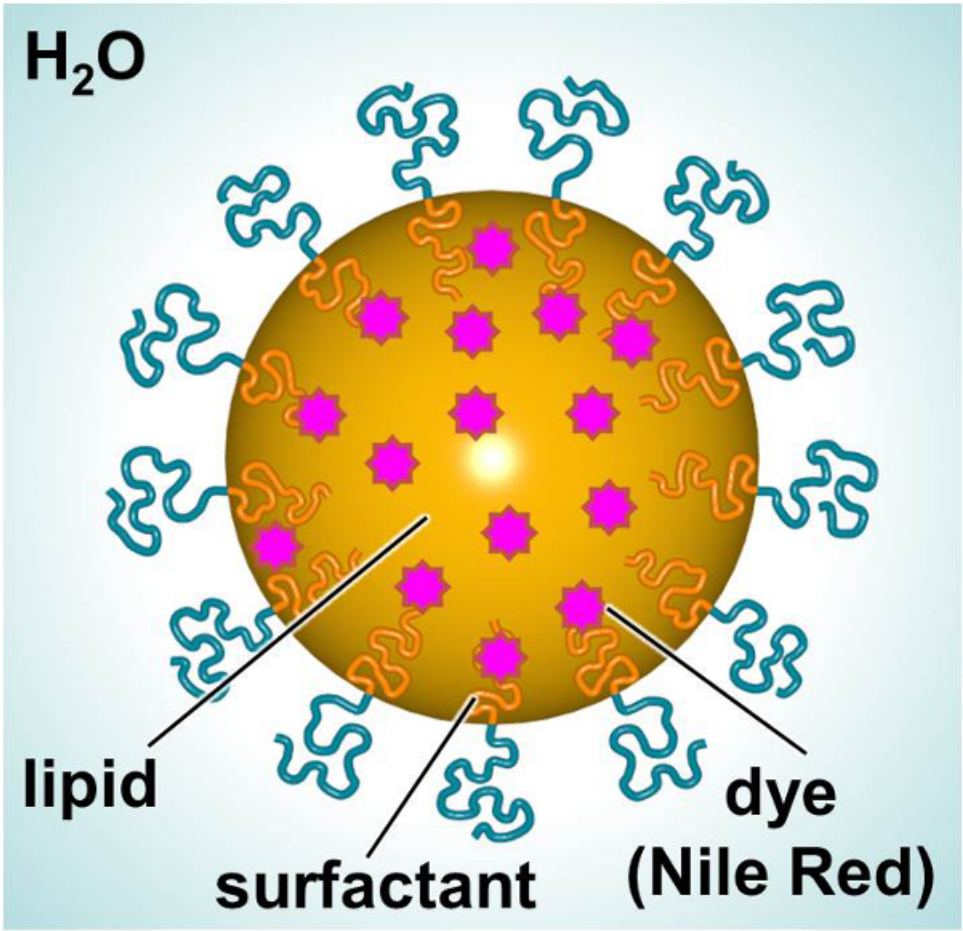

Figure 1. Schematic of SLN showing the major constituents. Please click here to view a larger version of this figure.

Protocol

1. Processing of SLNs

1. Synthesis of SLNs
   Note: Use the PIT method [1,17,20] to prepare the sub-20 nm SLNs [1].
   1. Use aseptic technique, bioreagents or cell culture grade reagents, and sterile materials (*i.e.*, pipettes, spatulas, vials, *etc.*).
   2. Use a biosafety cabinet for the synthesis of SLNs (**Figure 2**).
   3. Combine 0.6 mg of fluorescent dye (Nile Red (NiR), NiR concentration is approximately 0.3 mg/ml) and 0.10 g of Heneicosane (Lipid, 5 wt/wt% lipid concentration) into a vial (15 ml), co-melt at 90 °C, and stir.
   4. Add 0.11 g polyoxyethylene (10) oleyl ether (Surfactant, 5.5 wt/wt% surfactant concentration). Co-melt the resulting mixture at 90 °C and stir.
   5. Add 1.79 g of sterile water to the mixture, heat to 90 °C, and stir until a transparent nanoemulsion is formed.
      Note: Under continued stirring and controlled cooling, SLNs are created. These conditions cause an inversion of the water-in-oil emulsion to an oil-in-water emulsion. Lipophilic molecules such as NiR partition to the lipid droplets.
   6. Prepare a nanoemulsion in parallel without adding the fluorescent dye, in order to serve as a control sample. Combine 0.10 g of Heneicosane and 0.11 g polyoxyethylene (10) oleyl ether into a vial (15 ml) co-melt at 90 °C, and stir.

1. Add 1.79 g of sterile water to the mixture, heat to 90 °C, and stir until a transparent nanoemulsion is formed.

7. Further sterilize each nanoemulsion using a sterile 0.2 µm filter.

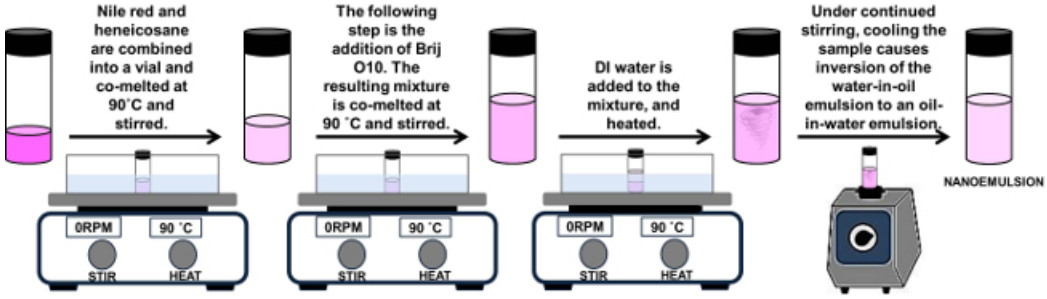

Figure 2. Schematic of synthesis of SLNs. Please click here to view a larger version of this figure.

2. Particle Size and Polydispersity
   1. Use dynamic light scattering (DLS) to measure the particle size and polydispersity of the SLNs [1] using a glass cuvette and an instrument designed to measure particle size.
   2. Prior to the measurements of the samples, measure the particle sizes of two known standards following the manufacturer's protocol for the standards preparation and measurement.
   3. Fill the glass cuvette with 1.5 ml of standard solution and measure the standard solution using the same measurement conditions as the samples.
      Note: Previous step was repeated for each standard.
   4. Measure the samples as prepared. For each, use the following experimental parameters: a run time of 100 sec, refractive index of water (1.33), viscosity of water at 20 °C (1.002 mPa·sec).
      Note: This technique uses frequency shifted light to measure the size of the nanoparticles.
   5. Report the average particle diameter and polydispersity of particle size distribution.

3. Melting Point and Latent Heat of Melting
   1. Use a differential scanning calorimeter (DSC) equipped with an auto-sampler and liquid nitrogen cooling source to investigate the thermal behavior of SLNs [1].
   2. Pipette the as-prepared SLNs into a 40 µl aluminum pan with a mass of approximately 25 mg and hermetically seal the pan using a universal crimper press to minimize moisture loss during the DSC scan.
   3. Measure each nanoemulsion from 5 to 80 °C.
   4. Report the melting point and the latent heat of melting from the DSC plot, where the valley represents the melting point and the integral of the area under the curve in the DSC plot divided by the amount of material represents the latent heat of melting.

2. SLNs Interaction with Fibroblasts and Dendritic Cells

1. Culture of Primary Human Fibroblasts
   1. Culture primary human fibroblasts according to the manufacturer's instructions in liquid medium for the culture of human dermal fibroblasts (medium 106), supplemented with the low serum growth supplement (LSGS) kit. Maintain cells in a humidified atmosphere at 37 °C, 5% CO_2 and subculture upon reaching 80% confluence.
   2. For both MTT and imaging analysis, seed cells in a 96-well plate, at a density of 2 x 10^4 cells per well, and allow to equilibrate at 37 °C O/N prior to SLN exposure.
   3. At time zero, dilute SLNs in complete medium as indicated (**Figure 4**), with respect to lipid concentration, and add 10 µl per well to each replicate well in the 96-well plate.
   4. Maintain cells at 37 °C, 5% CO_2, during the incubation period.

2. MTT Toxicity Assay
   1. After 24 hr of incubation with SLNs, determine cellular viability using the MTT assay, according to the manufacturer's protocol.
   2. Wash cells once and add fresh medium to each well (100 µl/well). Kill control wells by incubating in a 70% methanol solution for 10 min before replacing with fresh medium.
   3. Add MTT reagent (10 µl per well) to each well of the microplate and incubate O/N at 37 °C.
   4. After O/N incubation, solubilize intracellular formazin crystals with the provided detergent solution (100 µl per well) according to manufacturer's protocol.
   5. After 3 hr of incubation at RT, obtain absorbance values at a measurement wavelength of 570 nm using a microplate reader.
      Note: MTT reagent used should be less than 1% (w/v) 3-(4,5-dimethylthiazolyl-2)-2, 5-diphenyl-tetrazolium bromide.

3. Fluorescence Microscopy
   1. At specific time points following dosing of fibroblasts with SLN, wash the fibroblasts twice with sterile phosphate buffered saline (PBS) and fix for 10 min with cold 70% methanol.
   2. After 10 min, replace the methanol with PBS and capture images using an inverted microscope, using a band pass (BP) 690/50 nm filter set.

4. Culture of Mouse Bone Marrow Dendritic Cells

1. Induce mouse bone marrow-derived dendritic cells (BMDC) as previously described [23,24]. Briefly, plate single cell suspensions of C57BL/10 bone marrow in 100 mm Petri dishes at 2 x 10^6/plate with recombinant murine granulocyte-macrophage colony-stimulating factor (GM-CSF, 300 U/ml) and recombinant murine IL-4 (B cell stimulating factor, 200 U/ml). Change media every 3 days.
2. On day 7, add NiR-loaded SLNs to the dishes at a final concentration of 0.5 and 5.0 µg/ml lipid and maintain the cells in a 37 °C, 5% CO_2 incubator for the desired length of exposure.
3. Collect cells from the dishes by aspirating all the media in the plate, collecting it in a 50 ml tube, followed by thorough washing of the plate (to dislodge loosely adherent cells) with 5 ml of phosphate buffered saline (PBS) containing 4 mM ethylenediaminetetraacetic acid (EDTA). Collect the obtained cell suspension in the same 50 ml tube.

5. Assessment of SLNs Incorporation via Flow Cytometry
   1. Determine the concentration of the cell suspension obtained in point 2.4.3 and distribute 3x10^5 cells into a 12 mm x 75 mm round bottom FACS tube.
   2. Wash the cells by adding 1 ml of PBS and then centrifuging the tubes for 5 min at 400 x g, at a temperature of 4 °C.
   3. Discard the supernatant and resuspend the pellet with 100 µl of PBS/2 mM EDTA/0.1% bovine serum albumin (BSA) (staining buffer) containing anti-CD11c-FITC monoclonal antibody (0.25 µg/ml final). Incubate for 30 min on ice in the dark.
   4. Wash the cells with 1 ml of PBS and then centrifuge the tubes for 5 min at 400 x g, at a temperature of 4 °C.
   5. Discard the supernatant and resuspend each pellet with 400 µl of staining buffer. The cells are now ready for acquisition of the samples with a flow cytometer (possibly equipped with blue and red lasers).
   6. Using flow cytometry analysis software, assess the level of incorporation of SLNs by DC by gating on the population of CD11c+ cells (FITC positive) and comparing the intensity of SLNs-associated fluorescence (measured in the PerCP-Cy5.5 or APC channels).

Representative Results

The PIT method was used to synthesize the SLNs and the phase inversion temperature was determined utilizing a water bath. The samples were slowly heated and gently agitated until the solution appeared clear. The phase inversion temperature for the SLNs made using heneicosane lipid is 45 °C. **Table 1** summarizes the particle size, polydispersity, melting point and latent heat of melting for the SLNs. The SLNs synthesized using the processing conditions described above resulted in control SLNs and NiR-loaded SLNs with an average particle diameter of 18.59 and 16.87 nm and with a polydispersity of 5.83 and 4.47, respectively (**Figure 3**). The stability of the SLNs dispersion was monitored by the measurement of the particle size over 6 days at two different storage temperatures (4 and 23 °C). The particle size did not change over 6 days (data not shown).

The thermal behavior of the SLNs was investigated using differential scanning calorimetry. The synthesized SLNs have a melting point of 38.0 (± 0.4) and 36.8 (± 0.2) °C for the control SLNs and NiR-loaded SLNs, respectively. In contrast, the melting point for the bulk lipid is 40.0 °C, indicating the suppression of the melting point of the SLNs relative to the bulk lipid. As expected, the confinement to small dimensions and high surface area-to-volume ratio depress the nanoparticle melting point [1]. Moreover, the latent heat of melting for the control SLNs and NiR-loaded SLNs is 5.1 (± 0.2), and 4.0 (± 0.1) J/g, respectively. These results indicate that the level of crystallinity of the SLNs is affected by the payload, where the NiR-loaded SLNs showed a lower crystallinity in comparison with the control SLNs.

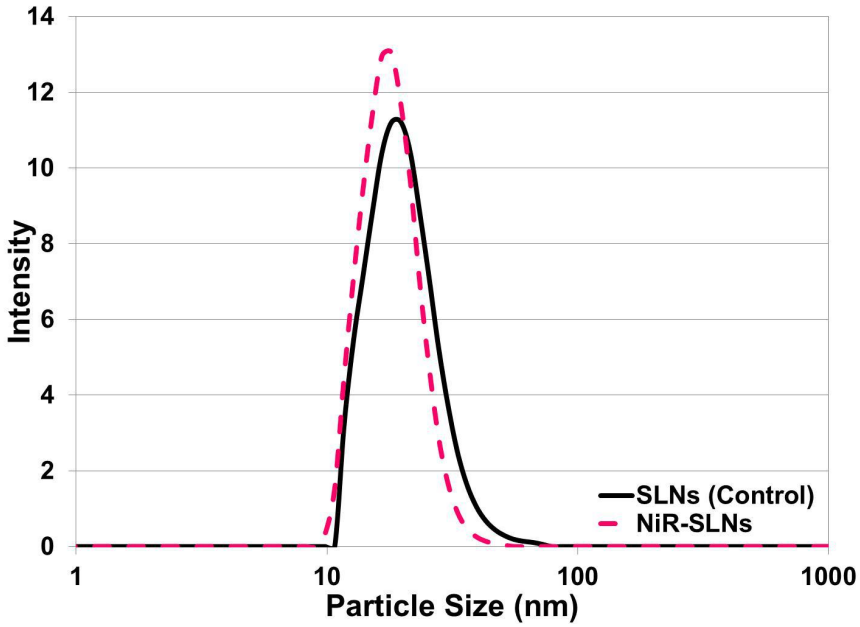

Figure 3. Particle size distribution of typical nanoemulsions. Please click here to view a larger version of this figure.

Sample	Particle Size (nm)	Polydispersity	Melting Point (°C)	Latent Heat of Melting (J/g)
SLNs (Control)	18.59	5.83	38.0 ± 0.4	5.1 ± 0.2

NiR-SLNs	16.87	4.47	36.8 ± 0.2	4.0 ± 0.1

Table 1. Summary of the physical properties and thermal behavior of the control SLNs and NiR-loaded SLNs including particle size, polydispersity, melting point and latent heat of melting.

In order to explore the interactions of particles and cellular models, the dose limitations of the SLN as directly applied to primary cells in culture, were first established. Using an MTT assay, the dose-response effect on cellular metabolism was measured, where increasing particle concentration resulted in a decrease in cellular viability (with respect to the untreated control cells). There was no observed difference in toxicity between cells exposed to SLN alone versus NiR-loaded SLN at these pre-determined doses. In parallel, cells were visually examined for adherence to the tissue culture polystyrene and images were taken to demonstrate both representative cellular morphology and the uptake of fluorescent particles over time (**Figure 5**). Using a dose equal to 5 µg/ml lipid (approximately 80% cellular viability) particle uptake was observed by 2 hr post exposure.

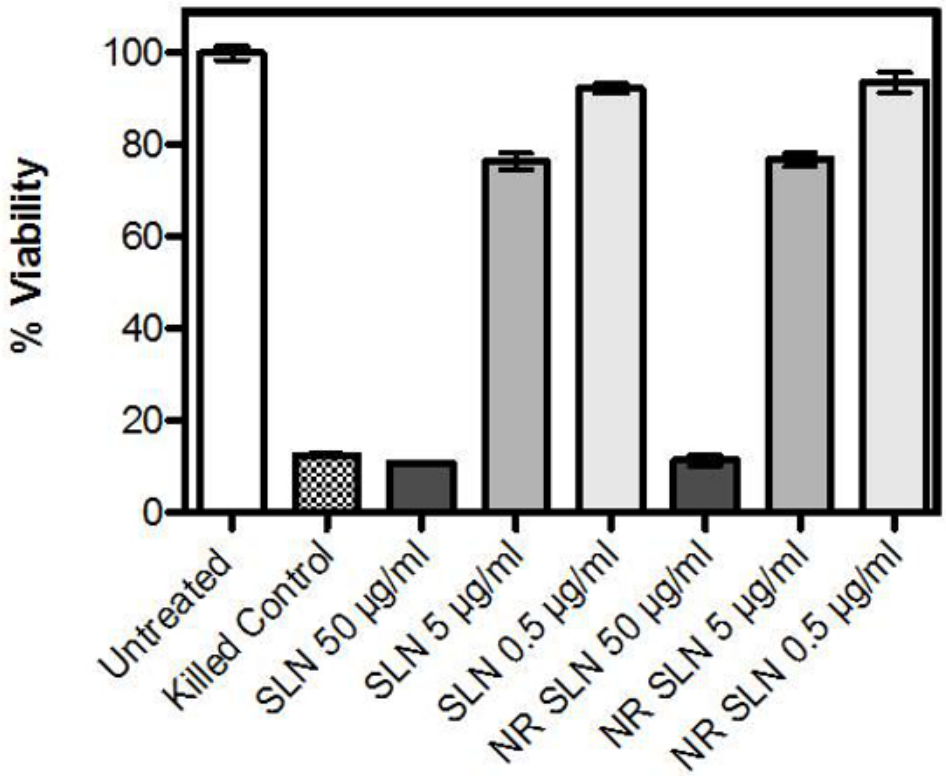

Figure 4. Viability of primary human dermal fibroblasts after 24 hr incubation with nanoparticles. Viability was measured using an MTT assay, and data represent percent viable cells with respect to untreated controls. Concentrations represent weight/volume lipid. Data reflect at least three independent experiments, performed in triplicate. Error bars indicate the standard error of the mean. Please click here to view a larger version of this figure.

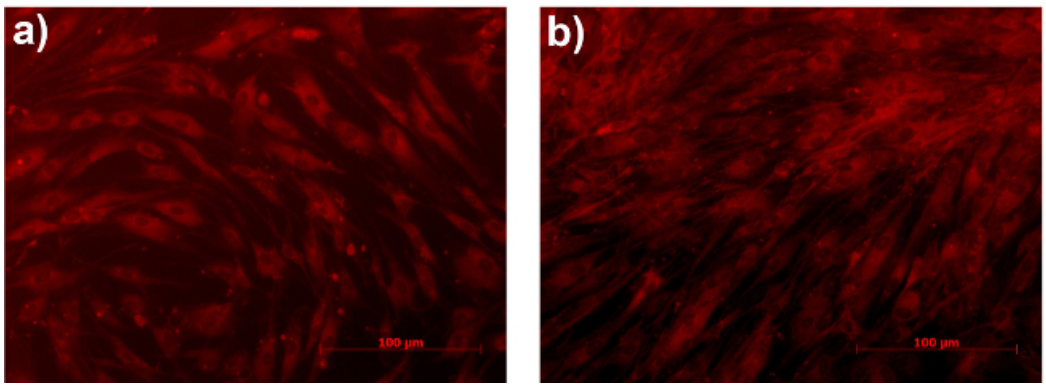

Figure 5. Primary human dermal fibroblasts after (A) 2 and (B) 24 hr incubation with NiR-loaded nanoparticles. Nanoparticle concentration is equal to 5 µg/ml lipid. Images are representative of at least three independent experiments, performed in duplicate. Please click here to view a larger version of this figure.

Based on the results of the dose limitation studies, the correlation between dose of SLNs and level of incorporation in murine BMDC was investigated. These cells are widely considered the best *in vitro* model of multiple DC subsets existing *in vivo* and allow for basic research level

investigations of both cellular and molecular effects of intended manipulations. BMDC were left untreated or exposed O/N to either 0.5 or 5.0 µg/ml lipid of the NiR-loaded SLNs (similarly to human fibroblast, use of 50 µg/ml lipid resulted in less than 10% viable cells) and the level of nanoparticle incorporation determined by measuring the intensity of NiR fluorescence in BMDCs via flow cytometry. A direct correlation between the concentration of SLNs used and the amount of fluorescence assessed in BMDCs was observed (**Figure 6A**). An analysis of the kinetic of NiR-loaded SLNs incorporation revealed a very rapid uptake by BMDC. The SLN fluorescent signal was already evident after 1 hr of exposure, while plateauing at around 5h of exposure (**Figure 6B**).

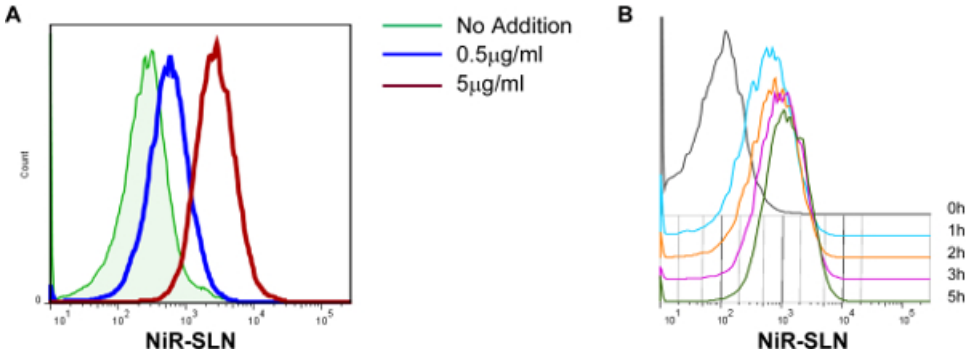

Figure 6. SLN incorporation by dendritic cells correlates with concentration of exposure. (A) Murine bone marrow-derived dendritic cells (BMDC) were exposed O/N to NiR-SLNs, at the concentration of lipid indicated, and the level of incorporation assessed via flow cytometry. Histogram overlays are all gated on the CD11c+ population. **(B)** Kinetic of SLN incorporation by BMDC. Cells were exposed to NiR-SLNs (5 µg/ml) for the indicated time and the level of fluorescence (on gated CD11c+ cells) was assessed by flow cytometry. Please click here to view a larger version of this figure.

Discussion

In this study, the synthesis of SLNs and their applicability for intracellular targeting applications were explored. These biocompatible nanoparticles have shown promise as delivery vehicles for multiple applications including drug delivery, gene silencing, and vaccine technologies [25-30]. Ultra-small SLNs were synthesized using a facile process, and their interactions with primary skin cells and primary immune cells were explored. SLNs were designed to include encapsulation of a fluorescent dye (NiR), which served as a model therapeutic cargo.

The PIT method was employed to synthesize SLN and the resulting particle properties (particle size, polydispersity, melting point, and latent heat of melting) were evaluated using dynamic light scattering and differential scanning calorimetry. Particle size and polydispersity analysis revealed the synthesis of ultra-small SLNs with narrow polydispersity, ideal for intracellular targeting applications. As previously reported, particle size can play an important role on cellular interactions [12]. The size of nanoparticles has been shown to have a dramatic effect, influencing uptake efficiency, internalization pathway selection, intracellular localization, and cytotoxicity [12]. Some of the overall trends with respect to cell-nanoparticle interactions documented in the literature include: critical size can vary with cell type and surface properties of the nanoparticles, and small nanoparticles have higher probability to be internalized by passive up-take than large ones [12]. Thermal analysis of the particles in this study revealed a different level of crystallinity (*i.e.,* latent heat of melting) between the control SLNs and those loaded with NiR dye. The crystallinity of the SLNs decreased due to the addition of the fluorescent dye, which acts as an impurity. The crystallinity of the therapeutic delivery system has been shown to be an important factor that affects the delivery and dose [31]. A decrease in crystallinity of the SLN vehicle can influence parameters such as therapeutic loading capacity and drug release kinetics [31]. The PIT method is a more gentle synthesis technique in comparison with other methods, with the limitation that only lipophilic drugs can be incorporated into the particles. Despite this limitation, SLNs synthesized using this method are highly biocompatible, making then suitable delivery platform for many applications in biomedical research.

The effects of SLN interaction on human dermal fibroblast viability were analyzed using an MTT assay. A dose-dependent decrease in viability was observed with increasing concentrations of SLN. During SLN synthesis, the lipid particles are stabilized with a surfactant layer. As the particle size decreases, surface area increases, as does the potential for cell surface interactions and cellular exposure to the surfactant layer, which may damage cell membranes. These experiments allowed the determination of the dosing concentration at which cellular uptake of particles could be observed while avoiding a significant decrease in cell viability due to membrane disruption. MTT analysis is a quantitative technique that can be broadly applied to understanding cellular health. In parallel, cells were examined using fluorescence microscopy in order to visualize the fluorescence of the cargo fluorescent dye, NiR. Using this technique, particle uptake was observed after only 2 hr of incubation with human fibroblasts. Fluorescence microscopy provides qualitative information related to cellular morphology and characteristics. Care must be taken to avoid excessive background staining and imaging of artifacts. In addition, as mouse models are generally the first choice for in depth cellular and molecular investigations, we analyzed the interaction between SLNs and murine cells. In particular, a great interest lies in the use of nanoparticles for the selective and controlled release of drugs that would modify the behavior of the immune system. Consequently, flow cytometry was employed to measure the uptake of particles by mouse dendritic cells. These data confirmed that phagocytic cells like dendritic cells can tolerate a similar range of SLNs concentration (with reduced viability observed at 50 µg/ml lipid as with human dermal fibroblasts) and the level of incorporation directly correlates with the concentration of SLN exposure. Moreover, DC revealed a very rapid incorporation of SLNs, suggesting that this population might represent a valuable target via SLN-mediated drug delivery.

This study includes the description of a method for the synthesis of ultra-small populations of biocompatible nanoparticles, as well as several *in vitro* methods by which to assess their cellular interactions. In future studies, additional assays may be employed to further characterize the particle-cell interactions and ultimately guide the successful development of therapeutic nanocarriers. These could include studies of drug release kinetics, analysis of cellular tropism, measurement of pro-inflammatory cytokine levels, and analysis of cellular transcriptomic changes over time.

Disclosures

The authors have nothing to disclose.

Acknowledgements

Research reported in this publication was supported by The Johns Hopkins Applied Physics Laboratory's Research and Exploratory Development Department, Office of Technology Transfer, and Stuart S. Janney Fellowship Program, in addition to the National Heart, Lung, and Blood Institute of the National Institutes of Health under Award Number R21HL127355.

References

1. Calderon-Colon, X. *et al.* Synthesis of sub-10 nm solid lipid nanoparticles for topical and biomarker detection applications. *J Nanopart Res.* **16** (2252), 1-10, (2014).
2. Patwekar, S. *et al.* Review on nanoparticles used in cosmetics and dermal products. *World Journal of Pharmacy and Pharmaceutical Sciences.* **3** (8), 1407-1421, (2014).
3. Martins, S. *et al.* Solid lipid nanoparticles as intracellular drug transporters: An investigation of the uptake mechanism and pathway. *International Journal of Pharmaceutics.* **430**, 216-227, (2012).
4. Yadav, N., Khatak, S., & Sara, U.V.S., Solid Lipid Nanoparticles - A Review. *International Journal of Applied Pharmaceuticals.* **5** (2), 8-18, (2013).
5. Weber, S., Zimmer, A., & Pardeike, J. Solid Lipid Nanoparticles (SLN) and Nanostructured Lipid Carriers (NLC) for pulmonary application: a review of the state of the art. *Eur J Pharm Biopharm.* **86** (1), 7-22, (2014).
6. Mahajan, A., Kaur, S., Grewal, N.K., & Kaur, S., Solid Lipd Nanoparticles (SLNs) - As Novel Lipd based Nanocarriers for Drugs. *International Journal of Advanced Research.* **2** (1), 433-441, (2014).
7. Buse, J., & El-Aneed, A. Properties, engineering and applications of lipid-based nanoparticle drug-delivery systems: current research and advances. *Nanomedicine (Lond).* **5**, 1237-1260, (2010).
8. Malam, Y., Loizidou, M., & Seifalian, A.M. Liposomes and nanoparticles: nanosized vehicles for drug delivery in cancer. *Trends Pharmacol Sci.* **30** (11), 592-599, (2009).
9. Lim, S.B., Banerjee, A., & Onyuksel, H. Improvement of drug safety by the use of lipid-based nanocarriers., *Journal of controlled release : official journal of the Controlled Release Society.* **163**, 34-45, (2012).
10. Ali Khan, A., Mudassir, J., Mohtar, N., & Darwis, Y. Advanced drug delivery to the lymphatic system: lipid-based nanoformulations. *International journal of nanomedicine.* **8**, 2733-2744, (2013).
11. Oussoren, C., & Storm, G. Liposomes to target the lymphatics by subcutaneous administration. *Advanced drug delivery reviews.* **50**, 143-156 (2001).
12. Shang, L., Nienhaus, K.., & Nienhaus, G.U. Engineered nanoparticles interacting with cells: size matters. *J Nanobiotechnology.* **12**, 5, (2014).
13. Joshi, M.D., & Muller, R.H. Lipid nanoparticles for parenteral delivery of actives. *European journal of pharmaceutics and biopharmaceutics : official journal of Arbeitsgemeinschaft fur Pharmazeutische Verfahrenstechnik e.V.* **71**, 161-172, (2009).
14. Torchilin, V.P. Micellar nanocarriers: pharmaceutical perspectives. *Pharmaceutical research.* **24**, 1-16, (2007).
15. Ashley, C.E. *et al.* The targeted delivery of multicomponent cargos to cancer cells by nanoporous particle-supported lipid bilayers. *Nature materials.* **10**, 389-397, (2011).
16. Patchan, M. *et al.* Nanobandage for controlled release of topical therapeutics. *Nanotech; Nanotechnology 2013: Bio Sensors, Instruments, Medical, Environment and Energy; Chapter 3: Materials for Dru., & Gene Delivery.* **3**, 255-258 (2013).
17. Forgiarini, A., Esquena, J., Gonzalez, C., & C, S. Formation and stability of nano-emulsions in mixed nonionic surfactant systems. *In: Koutsoukos P (ed) Trends in colloid and interface science XV, 118. Progress in Colloid and Polymer Science. Springer Berlin Heidelberg.* 184-189 (2001).
18. Nantarat, T., Chansakaow, S., & Leelapornpisid, P. Optimization, characterization and stability of essential oils blend loaded nanoemulsions by PIC technique for anti-tyrosinase activity. *International Journal of Pharmacy and Pharmaceutical Sciences.* **7**, 308-312 (2015).
19. Sevcikova, P., Vltavska, P., Kasparkova, V.., & Krejci, J. Formation, Characterization and Stability of Nanoemulsions Prepared by Phase Inversion. *Proceeding MACMESE'11 Proceedings of the 13th WSEAS international conference on Mathematical and computational methods in science and engineering.* 132-137 (2011).
20. Forgiarini, A., Esquena, J., Gonzalez, C., & Solans, C. Studies of the relation between phase behavior and emulsification methods with nanoemulsion formation. *In: Buckin V (ed) Trends in colloid and interface science XIV, 115. Progress in Colloid and Polymer Science. Springer Berlin Heidelberg.* 36-39 (2000).
21. Forgiarini, A., Esquena, J., Gonzalez, C., & Solans, C. Formation of nano-emulsions by low-energy emulsification methods at constant temperature. *Langmuir.* **17** (7), 2076-2083, (2001).
22. Cabone, C., Tomasello, B., Ruozi, B., Renis, M.., & Puglisi, G. Preparation and optimization of PIT solid lipid nanoparticles via statistical factorial design. *Eur J Med Chem.* **49**, 110-117, (2012).
23. Raimondi, G. *et al.* Mammalian Target of Rapamycin Inhibition and Alloantigen-Specific Regulatory T Cells Synergize To Promote Long-Term Graft Survival in Immunocompetent Recipients. *J Immunol.* **184**, 624-636, (2010).
24. Jhunjhunwala, S., Raimondi, G., Thomson, A.W.., & Little, S.R. Delivery of rapamycin to dendritic cells using degradable microparticles. *J Control Release.* **133** (13), 191-197, (2009).
25. Kapse-Mistry, S., Govender, T., Srivastava, R., & Yergeri, M. Nanodrug delivery in reversing multidrug resistance in cancer cells. *Front Pharmacol.* **5** (159), 1-22, (2014).
26. Musacchio, T.., & Torchilin, V.P. Recent developments in lipid-based pharmaceutical nanocarriers. *Front Biosci (Landmark Ed).* **1** (16), 1388-1412, (2011).

27. Cerpnjak, K., Zvonar, A., Gašperlin, M., & Vrečer, F. Lipid-based systems as a promising approach for enhancing the bioavailability of poorly water-soluble drugs. *Acta Pharm.* **63** (4), 27-445, (2013).
28. Rodrìguez-Gascòn, A., Pozo-Rodrìguez, A.., & Solinìs, M.A. Development of nucleic acid vaccines: use of self-amplifying RNA in lipid nanoparticles. *Int J Nanomedicine.* **9**, 1833-1843, (2014).
29. Almeida, A.J., & Souto, E. Solid lipid nanoparticles as a drug delivery system for peptides and proteins. *Adv Drug Deliv Rev.* **59**, 478-490, (2007).
30. Pardeshi, C. *et al.* Solid lipid based nanocarriers: an overview. *Acta Pharm.* **62**, 433-472 (2012).
31. Attama, A.A., Momoh, M.A., & Builders, P.F. in *Recent Advances in Novel Drug Carrier Systems.* (ed Sezer A. D.) Ch. Lipid Nanoparticulate Drug Delivery Systems: A Revolution in Dosage Form Design and Development, 107-140 (2012).

